BMC Medicine

RESEARCH

Open Access

Histological, histochemical, and immunohistochemical characterization of NANOULCOR nanostructured fibrin-agarose human cornea substitutes generated by tissue engineering

Olimpia Ortiz-Arrabal[1,2], Cristina Blanco-Elices[1,2], Carmen González-Gallardo[1,2,3], David Sánchez-Porras[1,2], Miguel Etayo-Escanilla[1,2], Paula Ávila Fernández[1,2], Jesús Chato-Astrain[1,2], Óscar-Darío García-García[1,2*], Ingrid Garzón[1,2*] and Miguel Alaminos[1,2]

Abstract

Background Human artificial corneas (HAC) generated by tissue engineering recently demonstrated clinical usefulness in the management of complex corneal diseases. However, the biological mechanisms associated to their regenerative potential need to be elucidated.

Methods In the present work, we generated HAC using nanostructured fibrin-agarose biomaterials with cultured corneal epithelial and stromal cells, and we compared the structure and histochemical and immunohistochemical profiles of HAC with control native corneas (CTR-C) and limbus (CTR-L) to determine the level of biomimicry of the HAC with these two native organs.

Results HAC tissues consisted of a stratified epithelium and a cellular stromal substitute. The interface between stroma and epithelium was similar to that of CTR-C, without the finger-shaped palisades of Vogt found in CTR-L, and contained a poorly developed basement membrane as determined by PAS histochemistry. Analysis of the stromal layer revealed that HAC contained significantly lower amounts of extracellular matrix components (collagen, proteoglycans, decorin, keratocan, and lumican) than CTR-C and CTR-L, with all samples being devoid of elastic and reticular fibers. At the epithelial level, HAC were strongly positive for several cytokeratins, although KRT5 was lower in HAC as compared to CTR-C and CTR-L. The expression of crystallin lambda was lower in HAC than in control tissues, whereas crystallin alpha-a was similar in HAC and CTR-C. No differences were found among HAC and controls for the cell–cell junction proteins CX43 and TJP1. When specific markers were analyzed, we found that HAC expression profile of KRT3, KRT19, KRT15, and ΔNp63 was more similar to CTR-L than to CTR-C.

*Correspondence:
Óscar-Darío García-García
ogarcia@ugr.es
Ingrid Garzón
igarzon@ugr.es
Full list of author information is available at the end of the article

Conclusions These results suggest that HAC generated in the laboratory could be structurally and functionally more biomimetic to the structure found at the corneal limbus than to the central cornea, and open the door to the use of these artificial tissues in patients with limbal deficiency.

Keywords Cornea, Tissue engineering, Limbal stem cells, Histology, Advanced therapies

Background

Numerous conditions, including trauma, infections, congenital malformations, degeneration, and other diseases, may affect the transparency of the human cornea and cause blindness [1]. Most of these diseases can be treated by cornea transplantation or keratoplasty. However, this technique is dependent on the availability of donors and is subjected to several limitations that make necessary the search for alternative treatments [2, 3].

In this milieu, tissue engineering techniques allow the development of human artificial corneas (HAC) able to reproduce the structure and physiology of the native cornea [4]. HAC have been generated to the date using different scaffolds, including, among others, the human amniotic membrane [5], decellularized tissues [6, 7], and different hydrogels such as type-I collagen, fibrin, or chitosan [7–9]. To generate a corneal epithelial layer on the surface of most HAC, researchers typically make use of limbal epithelial stem cells (LESCs) isolated from the scleral limbus and expanded in culture [10]. The reason for this is that mature epithelial cells in the central cornea are thought to be terminally differentiated and unable to proliferate and differentiate ex vivo, whereas LESCs have high proliferation potential and can generate large amounts of epithelial cells in culture. In fact, it is well known that LESCs are the stem cells in charge of maintaining corneal epithelial turnover and integrity, and central cornea epithelial cells derive from LESCs [11]. However, the microenvironment of LESCs and mature corneal epithelial cells is very different, and both cell types are known to be structurally and physiologically different [12].

One of the HAC models showing potential clinical usefulness is NANOULCOR, a nanostructured fibrin-agarose human anterior lamellar cornea consisting of human corneal cells and nanostructured fibrin-agarose biomaterials. This HAC showed promising preclinical results in laboratory animals [10, 13] and good biocompatibility and functionality in patients with severe corneal damage enrolled in a preliminary advanced therapies clinical trial [14].

In the present work, we evaluated a fibrin-agarose HAC model using an array of histological, histochemical, and immunohistochemical methods and compared the results with the human native scleral limbus and central cornea in order to determine the level of biomimicry of the HAC with these two native organs. This study could contribute to improve the clinical treatment of patients with severe corneal defects.

Methods

Cell isolation and culture

Primary cultures of human cornea stromal keratocytes and LESCs were obtained from samples of human limbal scleral rings as previously reported [13, 15]. Donor corneas were preserved at 31 °C until 30 days after donation, using tissue culture media at the corneal bank of Andalusia, following the protocols established by this bank, and limbal rings were provided after keratoplasty was carried out. Average age of the donors used in the present work was 51.5 ± 23 years. Stromal keratocytes were isolated by enzymatic digestion using a 2 mg/mL solution of *Clostridium histolyticum* type-I collagenase (Gibco-Thermo Fisher Scientific, Waltham, MA, USA) at 37 °C for 6 h and then cultured with Dulbecco's modified Eagle's medium (DMEM) supplemented with 10% fetal bovine serum (FBS) and 1% antibiotic-antimycotics solution (both from Merck, Burlington, MA, USA). LESCs were cultured in an epithelial medium consisting of a mixture of Ham-F12 (150 mL), DMEM (300 mL), and FBS (50 mL), supplemented with 1% antibiotic-antimycotics, adenine (24 μg/mL), insulin (5 μg/mL), triiodothyronine (1.3 ng/mL), hydrocortisone (0.4 μg/mL), and epidermal growth factor (EGF) (10 ng/mL) (all from Merck). In all cases, cells were cultured at 37 °C in a humidified incubator with 5.0% CO_2 using standard cell culture conditions. The culture medium was changed every 2–3 days, and cells were dissociated with 0.25% trypsin–EDTA (Merck) when 70% confluence was reached. Cells corresponding to the 3rd–4th cell passages were used to prevent cell senescence derived from long-term culturing.

This research was performed in accordance with guidelines and regulations of the Association for Research in Vision and Ophthalmology (ARVO) for the use of animals in ophthalmic and vision research. This project was approved by the local Human Research and Ethics Committee of the province of Granada (PEIBA) (numbers 1915-N-20 and 2224-N-20).

Generation of human artificial corneal substitutes (HAC)

HAC were generated using fibrin-agarose hydrogels with a final concentration of agarose of 0.1%, as previously reported [15, 16]. In brief, a biological substitute of the corneal stroma was first generated by mixing 3.8 mL of human plasma with 250 µL of a melted 2% solution of type-VII agarose in phosphate buffer saline (PBS) and 375 µL of DMEM containing 100,000 human keratocytes. To prevent gel fibrinolysis, the mixture was then supplemented with 75 µL of a 100 mg/mL solution of tranexamic acid (Amchafibrin™, Fides Ecopharma, Valencia, Spain), and 500 µL of 1% calcium chloride (Merck) was added at the final step to trigger the fibrin polymerization reaction. This mixture was rapidly aliquoted in Transwell cell culture inserts with 0.4 µm porous membranes (Sarstedt, Nümbrecht, Germany) and allowed to jellify at 37 °C for at least 6 h. Then, 500,000 cultured LESCs were added on top of the stromal substitutes to generate an epithelial layer [16]. HAC were kept in culture for 4 weeks, using the air–liquid culture technique from the third week to promote epithelial stratification and differentiation [15]. Finally, plastic compression nanostructuration was performed to improve the biomechanical properties of HAC, as previously reported [13, 16, 17]. The approximate thickness of the final product was 500 µm, as previously published [18], and its optical properties were described elsewhere [18–20]. In general, HAC showed approximately 80% of the light transmittance of the control native corneas [13].

Histological analyses

HAC and control human native corneas (CTR-C) and scleral limbi (CTR-L) tissues were fixed for 48 h in 4% formaldehyde and embedded in paraffin following standard histology laboratory protocols. Four micrometer-thick histological sections were obtained, placed on glass slides, deparaffinized with xylene, cleared in ethanol, and rehydrated in water. In order to analyze the histological structure of each sample, tissue sections were stained with hematoxylin–eosin (HE). In brief, sections were incubated for 3 min in hematoxylin (PanReac AppliChem, Barcelona, Spain), rinsed for 5 min in tap water, and stained with eosin (PanReac AppliChem) for 1 min. Samples were then washed in distilled water, dehydrated in alcohol series, and coverslipped. Histological images were obtained using a Pannoramic® DESK II DW scanner (3D Histotech, Budapest, Hungary).

Analysis of basement membrane and extracellular matrix (ECM) components by histochemistry

Deparaffinized tissue sections were subjected to several histochemical methods following previously published protocols [17, 21]. First, basement membrane glycosaminoglycans were stained using the periodic acid-Schiff (PAS) method. In brief, tissue sections were incubated in an oxidant 0.5% periodic acid solution for 5 min, incubated in Schiff reagent for 15 min, and slightly counterstained with Harris hematoxylin for 20 s. Then, relevant components of the extracellular matrix (ECM) were identified using specific histochemical techniques. Elastic fibers were stained with the method of Verhoeff (VER), consisting in a 10 min incubation in Verhoeff staining solution, followed by a brief differentiation in 2% ferric chloride. Reticular fibers were identified using the metal reduction protocol of Gomori (RET). In this case, sections were incubated in 1% potassium permanganate, followed by 2% sodium metabisulfite solution and sensibilization with 2% iron alum, incubation in ammoniacal silver and 20% formaldehyde. Differentiation was then performed with 2% gold chloride and 2% thiosulfate. To identify mature collagen fibers in the tissue ECM, we used the picrosirius red histochemical method (PSR), by incubating tissue sections for 30 min in sirius red F3B reagent, followed by Harris hematoxylin counterstaining for 5 min. ECM proteoglycans were assessed using the alcian blue histochemical method (AB). For this, sections were incubated for 30 min in AB solution, washed, and slightly counterstained with nuclear fast red solution for 1 min. All histochemical reagents were purchased from PanReac AppliChem.

Analysis of extracellular matrix (ECM) components and epithelial cell markers by immunohistochemistry and immunofluorescence

Specific components of the tissue ECM and markers of epithelial cells were identified in each sample by immunohistochemistry and immunofluorescence with specific primary antibodies. For cornea ECM components, fibrillar type-I collagen (COL-I) was analyzed, along with decorin (DCN), keratocan (KER), and lumican (LUM). At the epithelial level, we first analyzed globally the presence of cytokeratins using two cytokeratin cocktails (pancytokeratin (PCK) and AE1/AE3). Then, we evaluated the presence of cytokeratin 5 (KRT5), crystallin λ (CRYλ), crystallin alpha-a (CRYαa), connexin 43 (CX43), and tight junction protein 1 (TJP1). As specific markers of mature corneal epithelial cells found at the central cornea, we analyzed the presence of cytokeratin 3 (KRT3), whereas cytokeratin 19 (KRT19) and cytokeratin 15 (KRT15), the limbal isoform of the protein p63 (ΔNp63), were analyzed as specific markers of LESCs residing at the limbal area. All these analyses were carried out using triplicates ($n=3$ for each type of tissue).

On the one hand, COL-I, DCN, KER, LUM, PCK, AE1/AE3, KRT3, KRT5, KRT15, KRT19, CRYλ, and

ΔNp63 markers were detected by immunohistochemistry. Briefly, tissue sections were dewaxed and rehydrated, and then antigen retrieval was carried out at 95 °C. Endogenous peroxidase was blocked with 3% of H_2O_2 in PBS, and nonspecific antibody binding sites were blocked with 1×casein and normal horse serum (both, from Vector Laboratories, Burlingame, CA). Then, samples were incubated with primary antibodies overnight at 4 °C in a humid chamber following the technical details summarized in Additional file 1: Table S1. After washing with PBS, samples were incubated with ready-to-use secondary antibodies labeled with peroxidase for 1 h at room temperature (RT), and antibody binding was detected using a diaminobenzidine substrate kit (DAB) (both, from Vector Laboratories). Finally, samples were briefly counterstained with Harris hematoxylin. On the other hand, CRYαa, CX43, and TJP1 were analyzed by immunofluorescence. As described above for immunohistochemistry, tissue sections were dewaxed and rehydrated, and then antigen retrieval was performed at 95 °C. Unspecific sites were blocked with 1×casein and normal horse serum (both from Vector Laboratories) and samples were incubated with specific primary antibodies overnight at 4 °C in a humid chamber as detailed in Additional file 1: Table S1. Then, secondary antibodies conjugated with a fluorescent pigment (FITC or Cy3) were applied for 1 h at room temperature, and samples were counterstained with mounting medium with DAPI (Vector Laboratories). Images were obtained and analyzed using a Nikon Eclipse 90i fluorescence microscope.

Quantification and statistical analysis

Results obtained for the histochemical and immunohistochemical analysis of ECM components were quantified with the ImageJ software (National Institutes of Health, Bethesda, MD, USA), as previously described [21]. First, the staining intensity was calculated in each histological image for each analysis method giving a positive signal, by randomly selecting 15 points per sample type, and asking the software to calculate the signal staining intensity (INT). Then, we evaluated the percentage of area that was occupied by positively stained structures, by randomly selecting 15 square areas of 50×50 µm per sample type, and the area fraction (AF) was automatically assessed by the program. Results corresponding to the immunohistochemistry and immunofluorescence analysis of epithelial cell markers were semiquantitatively analyzed, as previously suggested [13, 16, 22]. In this case, the staining signal was categorized in each sample as negative (−), slightly positive (+/−), positive (+), very positive (++), or strongly positive (+++). These analyses were carried out by three independent expert histologists in order to reduce potential biases. A workflow describing the quantification process is shown in Fig. 1.

Quantitative results were compared among the three groups of study (CTR-C, CTR-L, and HAC). First, we

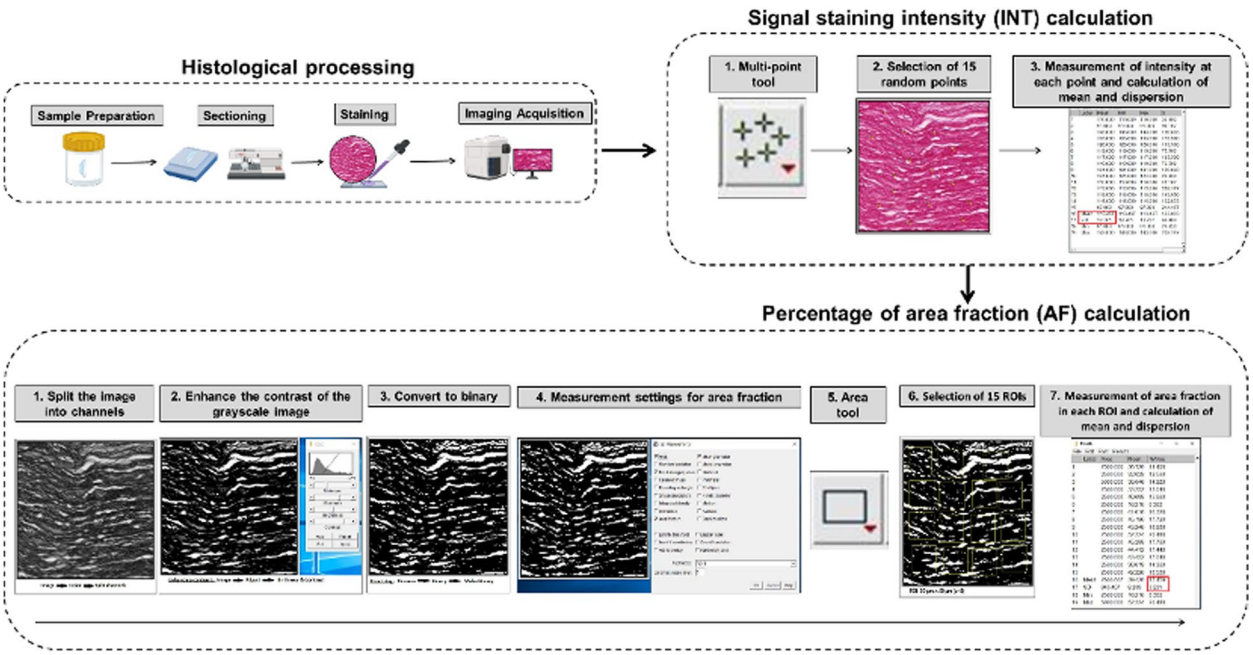

Fig. 1 Analysis of the histochemical staining signal in the different samples analyzed in the present work. Samples were fixed, embedded in paraffin, sectioned, and stained with each method, and the staining intensity was automatically quantified to determine both the signal intensity (INT) ant the area fraction (AF)

analyzed if each variable differed from a normal distribution using the Shapiro–Wilk test. As this test showed that most distributions were not normal, pairwise comparisons between two specific groups of study were carried out using the non-parametric test of Mann–Whitney. Statistical p values below 0.05 were considered statistically significant for the two-tailed test. Statistical testing was carried out using the Real Statistics Resource Pack software (Release 7.2) available at https://www.real-statistics.com/ (Purdue University, West Lafayette, IN, USA).

Results

Histological analysis

As shown in Fig. 2, the histological analysis of CTR-C using HE showed a stratified epithelium consisting of around 4–5 cell strata, in which basal cells displayed a typical columnar morphology, whereas apical cells were spindle-shaped, flattened, squamous cells. Analysis of CTR-L revealed the typical finger-shaped palisades of Vogt in which LESCs project towards the subjacent corneal stroma containing blood vessels. In addition, the histological analysis of HAC tissues revealed the presence of an epithelial layer with 5–6 cell strata, with cells displaying an elongated morphology showing very few differences among cell strata. When the stromal layer was analyzed, we found that both control tissues (CTR-C and CTR-L) consisted of a dense network of collagen fibers organized in thin lamellae containing disperse stromal keratocytes. In turn, HAC showed a randomly organized extracellular matrix of fibrin-agarose with abundant scattered keratocytes. No specialized structures, such as the Vogt palisades or blood vessels were found in HAC.

Analysis of the basement membrane using PAS histochemistry

When the different samples were stained with the PAS histochemical method, we found a PAS-positive signal at the interface between the epithelial and the stromal tissues of both the CTR-C and CTR-L, revealing the presence of a well-differentiated basement membrane at this level. When HAC tissues were analyzed, we found a positive staining of the epithelial cells, suggesting the presence of glycoproteins at this level, with a slight positive signal at the interface between the epithelial and the stromal layers, suggesting that HAC were devoid of a well-structured, mature basement membrane (Fig. 2).

Identification of corneal stroma ECM components by histochemistry and immunohistochemistry

On the one hand, we analyzed the presence of relevant fibrillar components of the corneal stroma ECM in control tissues and bioengineered corneas (Fig. 3). First, we found a negative staining signal for VHF and RET in CTR-C, CTR-L, and HAC, suggesting that elastic and reticular fibers were not present in these three tissues. Then, the analysis of collagen fibers was positive in all samples and was therefore quantified (Table 1). Quantification showed that of the results of the PSR histochemistry showed very strong staining signal intensity and area fraction (AF) in CTR-C, and very low signal in HAC,

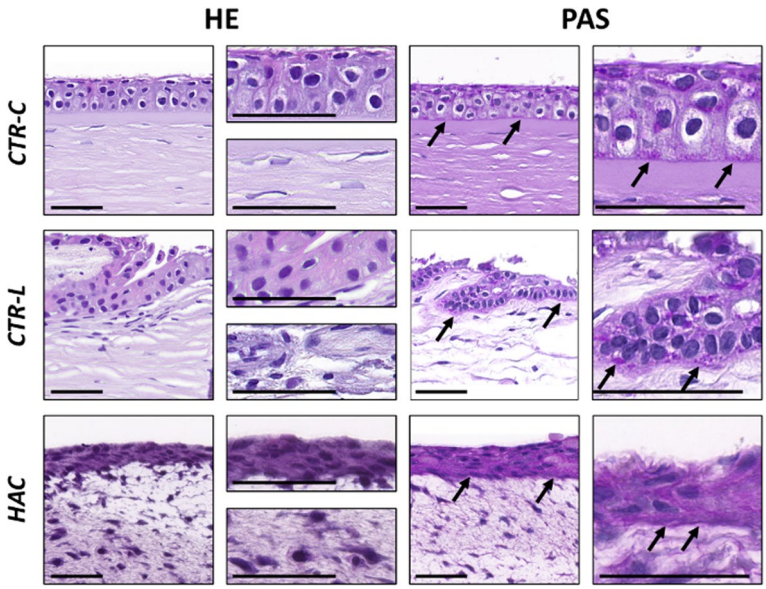

Fig. 2 Analysis of control human native corneas (CTR-C), control human native scleral limbi (CTR-L), and human artificial corneas (HAC) using hematoxylin–eosin (HE) and PAS histochemistry. Three samples were analyzed per type of tissue ($n = 3$). Images are shown at different magnifications for each method. Black arrows highlight illustrative PAS-positive areas in each sample. Scale bars: 50 µm

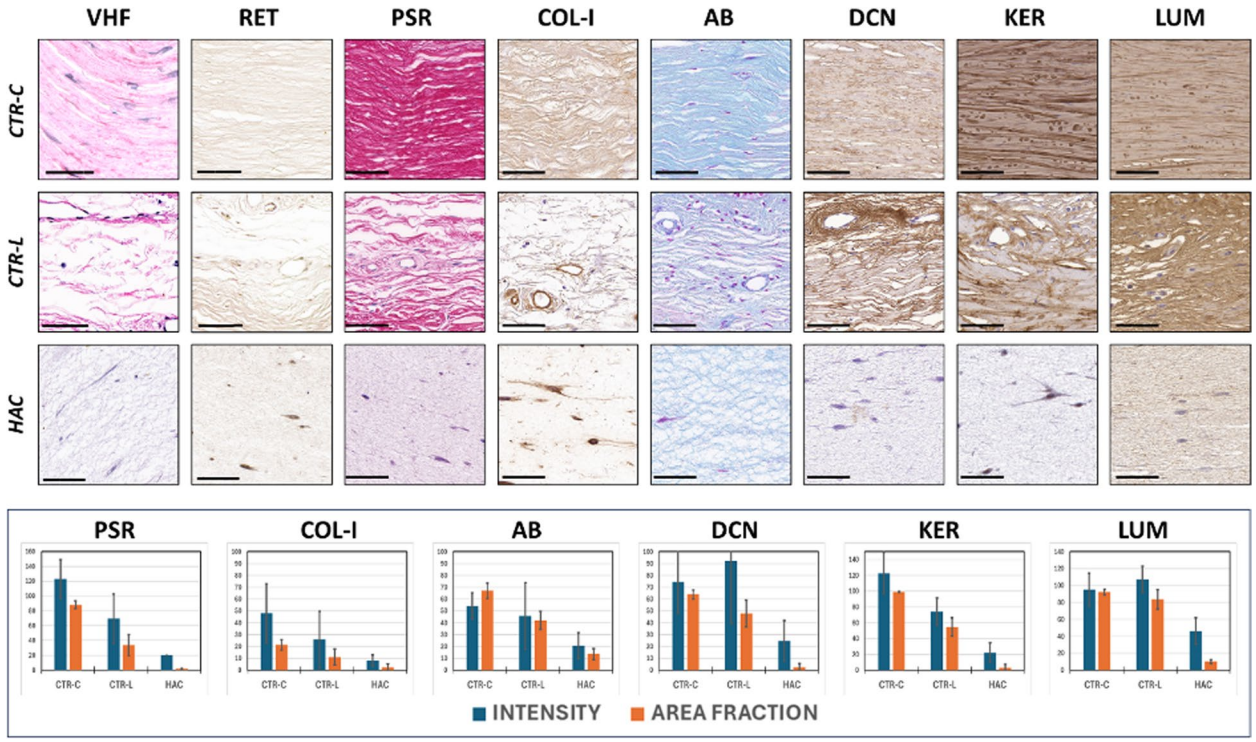

Fig. 3 Histochemical and immunohistochemical analysis of ECM components of the corneal stroma of control human native corneas (CTR-C), control human native scleral limbi (CTR-L), and human artificial corneas (HAC). Three samples were analyzed per type of tissue ($n = 3$). VHF, Verhoeff histochemistry for elastic fibers; RET, Gomori's reticulin histochemistry for the identification of reticular fibers; PSR, picrosirius red histochemical method for collagen fibers; COL-I, immunohistochemistry for type-I collagen; AB, alcian blue histochemistry for proteoglycans; DCN, immunohistochemistry for decorin; KER, immunohistochemistry for keratocan; LUM, immunohistochemistry for lumican. Top images correspond to histological microphotographs, whereas the signal quantification is represented, for those markers showing positive signal, in the lower panel. Scale bars: 50 μm

Table 1 Quantitative expression analysis of the ECM components showing a positive staining signal using histochemical and immunohistochemical methods in control human native corneas (CTR-C), control human native scleral limbi (CTR-L), and human artificial corneas (HAC). *INT*, signal intensity for each analysis method; *AF*, area fraction (percentage of tissue area occupied by positive signal for each analysis method). Columns to the left show averages and standard deviations, whereas statistical *p* values for the pairwise comparisons are shown to the right. *PSR*, picrosirius red histochemical method for collagen fibers; *COL-I*, immunohistochemistry for type-I collagen; *AB*, alcian blue histochemistry for proteoglycans; *DCN*, immunohistochemistry for decorin; *KER*, immunohistochemistry for keratocan; *LUM*, immunohistochemistry for lumican. Statistically significant differences are highlighted with asterisks (*)

		CTR-C	CTR-L	HAC	CTR-C vs. CTR-L	CTR-C vs. HAC	CTR-L vs. HAC
PSR	INT	122.93 ± 26.12	69.53 ± 33.08	20.00 ± 0.00	0.0001*	< 0.0001*	< 0.0001*
	AF	88.19 ± 5.25	33.76 ± 14.36	1.79 ± 0.90	< 0.0001*	< 0.0001*	< 0.0001*
COL-I	INT	48.07 ± 24.94	25.80 ± 23.99	8.20 ± 4.55	0.0164*	< 0.0001*	0.0367*
	AF	21.39 ± 4.27	11.05 ± 6.68	2.51 ± 2.85	0.0001*	< 0.0001*	< 0.0001*
AB	INT	54.13 ± 11.23	45.67 ± 27.99	20.60 ± 10.89	0.4363	< 0.0001*	0.0128*
	AF	67.06 ± 6.41	42.03 ± 7.63	13.50 ± 4.59	< 0.0001*	< 0.0001*	< 0.0001*
DCN	INT	74.47 ± 26.26	92.27 ± 52.63	24.87 ± 16.92	0.4124	< 0.0001*	0.0001*
	AF	63.80 ± 3.86	47.85 ± 11.25	2.49 ± 2.94	0.0002*	< 0.0001*	< 0.0001*
KER	INT	122.87 ± 26.16	74.13 ± 17.08	22.40 ± 12.16	< 0.0001*	< 0.0001*	< 0.0001*
	AF	99.08 ± 0.60	54.70 ± 11.59	2.86 ± 4.80	< 0.0001*	< 0.0001*	< 0.0001*
LUM	INT	95.33 ± 19.51	107.27 ± 15.67	46.2 ± 15.63	0.0675	< 0.0001*	< 0.0001*
	AF	92.24 ± 3.36	83.68 ± 11.46	10.27 ± 2.51	0.0453*	< 0.0001*	< 0.0001*

with CTR-L showing intermediate values. Differences were statistically significant for all pairwise comparisons. When type-I collagen was identified by immunohistochemistry, we also found that the highest intensity and AF values corresponded to CTR-C, followed by CTR-L, and the lowest results were found in HAC. Differences were statistically significant.

On the other hand, several non-fibrillar components of the corneal stroma ECM were identified by histochemistry and immunohistochemistry. As shown in Fig. 3 and Table 1, the analysis of tissue proteoglycans using AB revealed intense staining signal in CTR-C and CTR-L, with non-significant differences between both tissues for the staining intensity, although the area fraction was significantly higher in CTR-C. Both the CTR-C and CTR-L showed significantly higher intensity and AF than HAC. Then, we identified three specific ECM proteins using immunohistochemistry. For DCN, the highest intensity corresponded to CTR-C and CTR-L, with non-significant differences between both types of samples, and the highest intensity was found in HAC, with statistically significant differences with CTR-C and CTR-L. However, we found that the highest AF was found in DCN, followed by CTR-L and the lowest, in HAC, with differences among samples being statistically significant. For KER, our results revealed that the highest intensity and AF corresponded to CTR-C, with significant differences with CTR-L and HAC, and the lowest intensity and AF were found in HAC, with significant differences with CTR-C and CTR-L. Finally, our analysis showed that LUM intensity was very high in CTR-C and CTR-L, with non-significant differences between both types of samples, and the lowest intensity was found in HAC that was significantly lower than CTR-C and CTR-L. However, differences were statistically significant for the area fraction, with the highest values found in CTR-C, and the lowest, in HAC.

Analysis of epithelial cell markers

Epithelial characterization of the different samples analyzed in this work (Fig. 4 and Table 2) was first carried out by analyzing the presence of several non-specific cytokeratins by immunohistochemistry. In this milieu, the use of two pancytokeratin cocktails (PCK and AE1/AE3) confirmed the presence of global human cytokeratins in all samples, with very positive PCK signal in CTR-C and CTR-L and strongly positive signal in HAC, and strongly positive AE1/AE3 signal for all sample types. For KRT5, we found a strongly positive signal in CTR-C and CTR-L and a very positive signal in HAC. Then, we evaluated the presence of two corneal crystallins playing an important role in maintaining corneal transparency. For CRYλ, results were strongly positive for both control

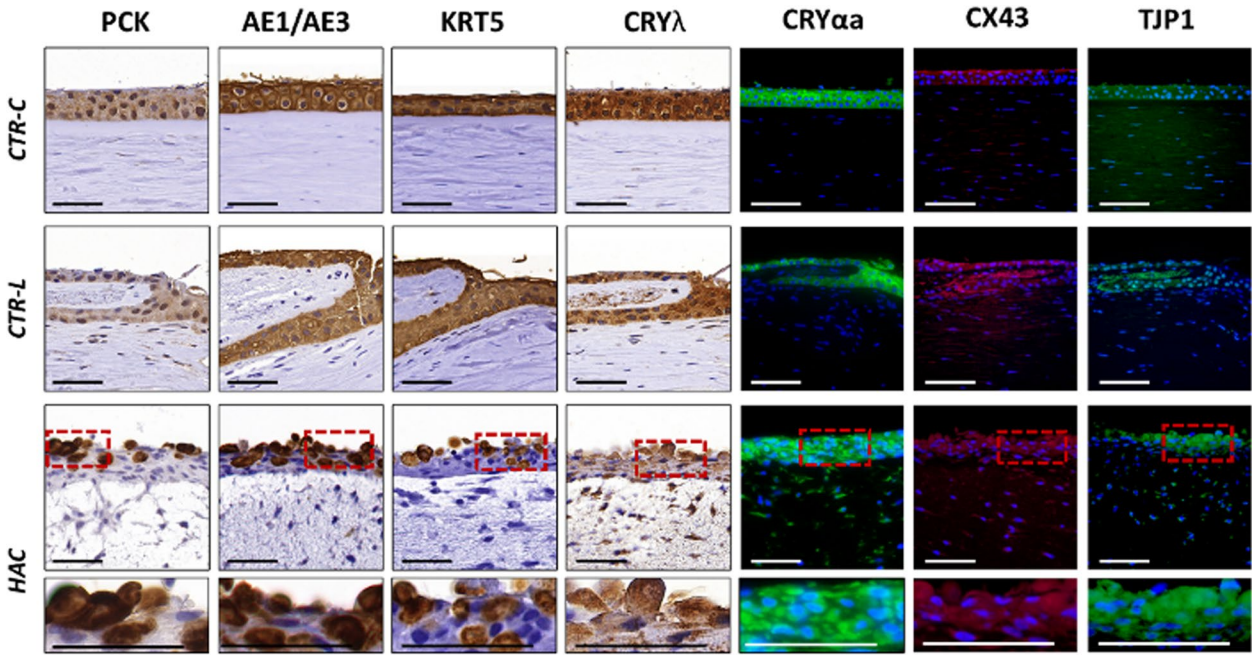

Fig. 4 Evaluation of epithelial cell markers in control human native corneas (CTR-C), control human native scleral limbi (CTR-L), and human artificial corneas (HAC) using immunohistochemistry and immunofluorescence. Three samples were analyzed per type of tissue ($n = 3$). PCK, human cytokeratin cocktail pancytokeratin; AE1/AE3, human cytokeratin cocktail AE1/AE3; KRT5, cytokeratin 5; CRYλ, crystallin λ; CRYαa, crystallin alpha a; CX43, connexin 43; TJP1, tight junction protein 1. Higher magnification inserts at the bottom of the image correspond to the areas highlighted with dotted red squares in the HAC tissues. Scale bars: 50 μm

Table 2 Results of the semiquantitative expression analysis of relevant epithelial cell markers in control human native corneas (CTR-C), control human native scleral limbi (CTR-L), and human artificial corneas (HAC) using immunohistochemistry and immunofluorescence. *PCK*, human cytokeratin cocktail pancytokeratin; *AE1/AE3*, human cytokeratin cocktail AE1/AE3; *KRT5*, cytokeratin 5; *CRYλ*, crystallin λ; *CRYαa*, crystallin alpha a; *CX43*, connexin 43; *TJP1*, tight junction protein 1; *KRT3*, cytokeratin 3; *KRT19*, cytokeratin 19; *KRT15*, cytokeratin 15; *ΔNp63*, limbal isoform of the protein p63. The staining signal was assessed as negative (−), slightly positive (+/−), positive (+), very positive (++), or strongly positive (+++)

	CTR-C	CTR-L	HAC
PCK	++	++	+++
AE1/AE3	+++	+++	+++
KTR5	+++	+++	++
CRYλ	+++	+++	++
CRYαa	+++	++	+++
CX43	++	++	++
TJP1	++	++	++
KRT3	+++	+	+/−
KRT19	+	++	++
KRT15	-	++	++
ΔNp63	+	++	++

tissues (CTR-C and CTR-L), whereas HAC showed very positive staining signal. For CRYαa, the signal was strongly positive in CTR-C and HAC and very positive in CTR-L. Finally, the analysis of two relevant cell–cell junction proteins (CX43 and TJP1) revealed a very positive signal in the three types of tissues analyzed here (CTR-C, CTR-L, and HAC).

Analysis of specific markers of mature epithelial cells and LESCs

When the expression of the corneal epithelium cell marker KRT3 was evaluated in the three types of tissues, we found a strongly positive signal at the epithelial layer of CTR-C, a positive signal at the origin of the limbal niche of CTR-L, with negative signal in the cells corresponding to the Vogt palisades, and a slightly positive signal in the epithelium of HAC tissue substitutes (Fig. 5 and Table 2).

Then, we evaluated several specific markers of LESCs using immunohistochemical and immunofluorescence methods (Fig. 5 and Table 2). Results of this analysis showed that KRT19 was positive in CTR-C and a very positive in CTR-L and HAC. For KRT15, signal was negative in the epithelial cells of the CTR-C and very positive in CTR-L and HAC. Finally, our analysis of the limbal stem cell marker ΔNp63 using immunofluorescence

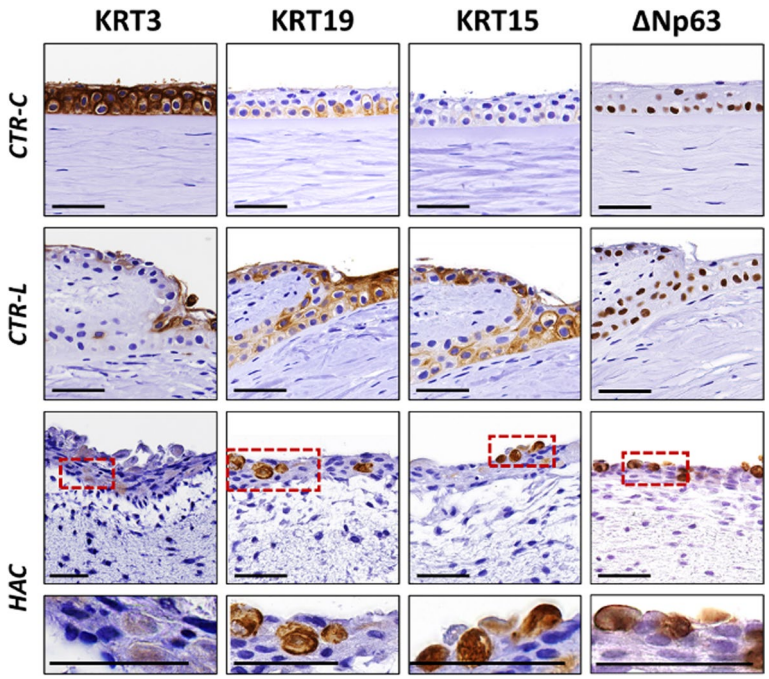

Fig. 5 Analysis of specific markers of the epithelial cells of the human cornea and limbus in control human native corneas (CTR-C), control human native scleral limbi (CTR-L), and human artificial corneas (HAC) using immunohistochemistry. Three samples were analyzed per type of tissue ($n=3$). KRT3, cytokeratin 3; KRT19, cytokeratin 19; KRT15, cytokeratin 15; ΔNp63, limbal isoform of the protein p63. Higher magnification inserts at the bottom of the image correspond to the areas highlighted with dotted red squares in the HAC tissues. Scale bars: 50 μm

showed positive signal in CTR-C and a very positive signal in CTR-L and HAC.

Discussion

The recent development of novel advanced therapies medicinal products allowed the regenerative treatment of severe diseases for which a curative therapy has not been described [23]. In the field of ophthalmology, corneal conditions affecting the structure of this organ are very difficult to manage, and novel alternative treatments are in need. In this context, the use of the NANOULCOR advanced therapies medicinal product (ATMP) offered promising results in one of the first clinical trials carried out in Europe with a bioartificial cornea substitute consisting of the two most external layers of the cornea—epithelium and stroma [17]. Although the results of this clinical trial have been positive, evaluation of the molecular mechanisms associated to the clinical efficiency of ATMPs used clinically is necessary for a proper characterization of these products.

One of the unsolved questions related to the clinical effectiveness of NANOULCOR is whether this ATMP retain the undifferentiation phenotype of LESCs, or if this product resembles the differentiated status of the human mature central cornea. Although this HAC was generated with cultured LESCs, it has been demonstrated that organotypic culture systems used during fabrication of NANOULCOR are able to induce partial cell differentiation [13, 15].

In the present work, we first demonstrated that the bioartificial tissues generated by tissue engineering reproduced the histological structure of the central cornea and were devoid of the Vogt palisades found in CTR-L. In fact, HAC consisted of a stromal substitute with a stratified epithelium on top, and the interface between both tissues was flat, in agreement with our previous publications [10, 16, 17], and as known for the normal central cornea [24]. When the basement membrane was analyzed, we confirmed our previous results suggesting that an incipient structure was present in HAC kept in culture, and exposition to the in vivo environment is required for the terminal differentiation of this basement membrane [17].

To determine the degree of biomimicry of HAC, and their similarity to control tissues, we then analyzed some relevant components of the human cornea stroma ECM. For the fibrillar components, we found that both the native tissues and the HAC were devoid of reticular and elastic fibers. These findings are not surprising, since the fine and definite structure of the corneal layers is crucial for a proper transparency [25], and the presence of thick non-collagenous fibers, especially the elastic fibers, could impair corneal transparency. It has been demonstrated that the human native cornea has elastic properties [26]. However, the presence of elastic fibers in the human cornea has not been described, and some reports suggest that corneal elasticity may be associated to elastin-free microfibril bundles [27]. Previous studies from our group also showed that HAC are devoid of fibrillar and elastic fibers [16, 17]. However, all tissues analyzed in the present work were rich in collagen fibers, especially the native CTR-C. It is well known that the corneal stroma consists of abundant well-organized of collagen fibrils arranged in the corneal stroma, and this structure is crucial for corneal transparency [25]. In contrast, several authors found that the collagen fibers number, concentration, and organization is significantly reduced in the sclero-corneal limbus [25], as found in our study. Finally, the lowest amount of collagen fibers corresponded to HAC. These results are in agreement with our previous findings demonstrating that cornea substitutes kept in culture show very low collagen contents that cannot be detected using histochemistry, and only very sensitive immunohistochemical methods can identify this fibers in HAC kept ex vivo [16]. These previous reports also demonstrated that in vivo grafting was able to significantly increase the presence of collagen fibers [17].

For the non-fibrillar components of the ECM, our results showed that HAC contained significantly lower amounts of proteoglycans, decorin, keratocan, and lumican than CTR-C and CTR-L, whereas all these components, except for keratocan, were similar in CTR-C and CTR-L. Again, these results coincide with previous reports suggesting that the bioartificial tissues kept in culture tend to show very low differentiation levels and express low amounts of these non-fibrillar components, whereas HAC implanted in vivo in laboratory animals significantly increased these components as a result of the in vivo environment and stromal-epidermal interaction [13, 17]. These results imply that the HAC generated in this work significantly differed from CTR-C and CTR-L in terms of ECM composition, suggesting that the stromal layer of these artificial tissues could be very undifferentiated. However, the lack of blood vessels and palisades of Vogt in HAC suggests that bioengineered corneas could morphologically more similar to CTR-C than CTR-L.

On the other hand, we analyzed the epithelial layer of HAC and compared their immunohistochemical and immunofluorescence profile with the control tissues. First, we found that HAC were able to express high amounts of non-specific cytokeratins, as it was the case of CTR-C and CTR-L. Keratins are essential elements of the cytoskeleton of human epithelial cells [28], and their presence in HAC confirms that epithelial layer of artificial corneas retains certain differentiation profile. In

addition, the positive expression of KRT5, a marker of epithelial cell proliferation [29], confirms that the epithelial layer of HAC retained proliferative and regenerative potential, as it is the case of control epithelia. Furthermore, we found that HAC epithelium was able to express relevant epithelial markers with a role in the human cornea and limbus, such as crystallins λ and αa, and the cell–cell junction proteins CX43 and TJP1. Crystallins are important proteins controlling light dispersion, and its presence in the human cornea is crucial for an appropriate transparency of this organ [30]. In the present work, we have analyzed the presence of two relevant crystallins (CRY-αa and CRY-λ) that were previously found expressed at high levels in the human native cornea and in artificial corneas generated by tissue engineering [16], but future studies should determine the presence of other crystallins expressed at lower level in the human cornea, such as CRY-β or CRY-ζ.

In general, very few differences were found between HAC epithelium and control tissues for all these epithelial cell markers, suggesting again that the epithelial layer of HAC retained its epithelial phenotype, at least until certain extent, as previously demonstrated for artificial corneas kept ex vivo [15–17].

Finally, we assessed the expression of some specific markers of the central cornea and limbus epithelial cells. By doing so, we found that KRT3, a specific cytokeratin of central cornea epithelium that is not expressed by LESCs [31], was mostly negative in HAC epithelium, whose cells showed very low expression of this corneal marker. Additionally, the specific markers of corneal limbus analyzed in this work (KRT15, KRT19, and ΔNp63) were found positively expressed not only in CTR-L, but also in the epithelial layer of HAC. As previously reported, KRT15 and KRT19 were expressed by the native human limbus, whereas the central cornea contains low amounts of these markers and high KRT3 expression [32]. In our work, we found that the epithelial layer of HAC showed high expression of KRT15 and KRT19, with a low signal for KRT3. Although further research is in need, we might hypothesize that the differentiation phenotype of HAC could resemble the corneal limbus, rather than the central cornea epithelium. Moreover, the high expression of the LESCs marker ΔNp63 in HAC epithelium at similar levels to CTR-L confirms the idea that HAC epithelium could functionally resemble the epithelial cells found at the limbus and could most likely retain the functions of this structure. Although the exact function of ΔNp63 in LESCs has not been elucidated, it has been demonstrated that this marker is highly specific of limbal cells, and its expression can be used to identify LESCs and differentiate these cells from those of the central cornea [33–35]. Future time-course studies should determine the stability of ΔNp63, along with other stem cell markers such as ABCG2 [36] in HAC epithelium of corneas kept ex vivo for longer periods of time.

In summary, our findings reveal that the HAC generated in the present work are partially differentiated, especially at the epithelial level, and could share some structural and functional similarities with both CTR-C and CTR-L. Morphologically, the relatively simple structure of HAC could be more biomimetic to the central cornea. However, the presence of the limbal markers KRT15, KRT19, and ΔNp63 suggests that HAC epithelium could be functionally similar to the limbus. The low expression of the central cornea marker KRT3 confirms that the epithelial cells in HAC preserve their stemness and differentiation potential and show only a limited differentiation profile while kept in culture. These results are in agreement with previous findings demonstrating that corneal substitutes kept in culture show partial differentiation profiles, and the use of air–liquid culture techniques can only in part increase epithelial differentiation and induce a limited expression of specific markers [15, 37]. However, terminal differentiation and maturation typically requires in vivo grafting and epithelial-stroma interaction [15–17]. Another factor influencing cell phenotype of bioartificial tissues kept in culture is the physical behavior of these tissues, especially regarding the thickness of the stromal layer and the biomechanical properties of these products [38]. In this milieu, previous studies from our group demonstrated that biomechanical properties are able to influence cell differentiation of human keratocytes used in cornea tissue engineering [18].

Although NANOULCOR was previously evaluated in rabbits using anterior lamellar keratoplasty [10, 13, 17], one of the limitations of the present study is the lack of in vivo studies in animal models of limbal stem cell deficiency to determine the potential usefulness of these HAC in patients with limbal damage. In addition, future studies should be carried out to compare NANOULCOR with other previously established models showing clinical efficacy, such as HOLOCLAR, in which cells were cultured on amniotic membrane scaffolds [39]. As a bilayered corneal substitute containing not only epithelial cells, but also a stromal substitute with keratocytes, we might hypothesize that NANOULCOR could have improved regenerative properties in patients with corneal stroma damage, such as severe corneal ulcers. Future clinical trials should determine the clinical potential of this HAC as compared to other cornea substitutes.

These findings may have several implications. On the one hand, the expression of different markers of epithelial differentiation in HAC epithelium may explain the positive results obtained in patients and the excellent biocompatibility found when NANOULCOR is grafted

at the corneal surface [14]. On the other hand, the fact that HAC could be functionally more similar to the human limbus than to central cornea may explain the regenerative potential of these artificial tissues.

Conclusions

As HAC epithelial cells could exert the same regenerative properties of the human limbus, our results suggest that HAC could support and maintain epithelial proliferation and corneal regeneration, as described for the native limbus [40]. In consequence, we may state that these bioartificial tissues could be used clinically for diverse applications requiring not only a successful regeneration of the corneal stroma, but also a reestablishment of the normal turnover and physiology of the corneal epithelium.

Abbreviations

AB	Alcian blue histochemical method
ABCG2	Transporter protein member 2 of ATP-binding cassette superfamily G
AE1/AE3	Pancytokeratin marker
AF	Area fraction
ATMP	Advanced therapies medicinal product
COL-I	Type-I collagen
CRYαa	Crystallin alpha-a
CRYλ	Crystallin λ
CTR-C	Control native corneas
CTR-L	Control native limbus
CX43	Connexin 43
DAB	Diaminobenzidine
DAPI	4′,6-Diamidino-2-fenilindol
DCN	Decorin
DMEM	Dulbecco's modified Eagle's medium
ECM	Extracellular matrix
EDTA	Ethylenediaminetetraacetic acid
EGF	Epidermal growth factor
FBS	Fetal bovine serum
HAC	Human artificial corneas
HE	Hematoxylin-eosin
INT	Signal staining intensity
KER	Keratocan
KRT15	Cytokeratin 15
KRT19	Cytokeratin 19
KRT3	Cytokeratin 3
KRT5	Cytokeratin 5
LESCs	Limbal epithelial stem cells
LUM	Lumican
PAS	Periodic acid-Schiff
PBS	Phosphate buffer saline
PCK	Pancytokeratin cocktail
PSR	Picrosirius red histochemical method
RET	Gomori's metal reduction method
RT	Room temperature
TJP1	Tight junction protein 1
VER	Verhoeff histochemical method
ΔNp63	Limbal isoform of the protein p63

Supplementary Information

The online version contains supplementary material available at https://doi.org/10.1186/s12916-024-03759-4.

Additional file 1: Table S1. Antibodies and experimental conditions used for the immunohistochemical analyses carried out in the present work.

Acknowledgements

The authors thank Fabiola Bermejo and the Experimental Unit for technical support with the histological analyses.

Authors' contributions

The authors contributed to this work as follows OOA, CBE, CGG, DSP, MEE, PAF, JCA, ODG, IG, and MA all contributed significantly to the conception, design, and execution of the study. OOA, CBE, IG and DSP were involved in the acquisition and analysis of data. JCA, ODG, IG, and MA provided critical input and expertise throughout the experimental process. All authors contributed to the interpretation of results and drafting of the manuscript.

Funding

Supported by Instituto de Salud Carlos III (ISCIII), Ministry of Science, Innovation and Universities, grants FIS PI23/00335, FIS PI20/00317, and ICI21/00010 (NANOULCOR). Supported by grant CSyF PI-0086–2020 from Consejería de Salud y Consumo, Junta de Andalucía, Spain and grant B-CTS-504-UGR20 (Programa Operativo FEDER Andalucía 2014-2020, University of Granada and Consejería de Universidad, Investigación e Innovación). Cofinanced by the European Regional Development Fund (ERDF) through the "Una manera de hacer Europa" program.

Data availability

The data supporting the findings of this study are openly available in the public repository Zenodo at https://zenodo.org/records/10845879, with the DOI number 10.5281/zenodo.10845879 with the license Creative Commons Attribution 4.0 International [41].

Declarations

Competing interests

The authors declare no competing interests.

Author details

[1]Department of Histology, Tissue Engineering Group, School of Medicine, University of Granada, Granada, Spain. [2]Instituto de Investigación Biosanitaria ibs.GRANADA, Granada, Spain. [3]Division of Ophthalmology, University Hospital Clínico San Cecilio, Granada, Spain.

Received: 7 June 2024 Accepted: 7 November 2024
Published online: 13 November 2024

References

1. Jhanji V, Billig I, Yam GHF. Cell-free biological approach for corneal stromal wound healing. Front Pharmacol. 2021;12:671405.
2. Gain P, Jullienne R, He Z, Aldossary M, Acquart S, Cognasse F, et al. Global survey of corneal transplantation and eye banking. JAMA Ophthalmol. 2016;134:167–73.
3. Bremond-Gignac D, Copin H, Benkhalifa M. Corneal epithelial stem cells for corneal injury. Expert Opin Biol Ther. 2018;18:997–1003.
4. Guérin LP, Le-Bel G, Desjardins P, Couture C, Gillard E, Boisselier É, et al. The human tissue-engineered cornea (hTEC): recent progress. Int J Mol Sci. 2021;22:1291.
5. Leal-Marin S, Kern T, Hofmann N, Pogozhykh O, Framme C, Börgel M, et al. Human amniotic membrane: a review on tissue engineering, application, and storage. J Biomed Mater Res B Appl Biomater. 2021;109:1198–215.
6. Oliveira AC, Garzón I, Ionescu AM, Carriel V, Cardona J de la C, González-Andrades M, et al. Evaluation of small intestine grafts decellularization methods for corneal tissue engineering. PLoS ONE. 2013;8:e66538.
7. Rodríguez-Lorenzo LM, Reyes-Ortega F, Griffith M. Editorial: biomaterials used in tissue engineering for the restoration of ocular disorders. Front Pharmacol. 2024;15:1369505.
8. Sklenářová R, Akla N, Latorre MJ, Ulrichová J, Franková J. Collagen as a biomaterial for skin and corneal wound healing. J Funct Biomater. 2022;13:249.
9. Lyu Y, Liu Y, He H, Wang H. Application of silk-fibroin-based hydrogels in tissue engineering. Gels. 2023;9:431.

10. Rico-Sánchez L, Garzón I, González-Andrades M, Ruíz-García A, Punzano M, Lizana-Moreno A, et al. Successful development and clinical translation of a novel anterior lamellar artificial cornea. J Tissue Eng Regen Med. 2019;13:2142–54.
11. Tavakkoli F, Eleiwa TK, Elhusseiny AM, Damala M, Rai AK, Cheraqpour K, et al. Corneal stem cells niche and homeostasis impacts in regenerative medicine; concise review. Eur J Ophthalmol. 2023;33:1536–52.
12. Soleimani M, Cheraqpour K, Koganti R, Baharnoori SM, Djalilian AR. Concise review: bioengineering of limbal stem cell niche. Bioengineering (Basel). 2023;10:111.
13. Garzón I, Chato-Astrain J, González-Gallardo C, Ionescu A, Cardona J de la C, Mateu M, et al. Long-term in vivo evaluation of orthotypical and heterotypical bioengineered human corneas. Front Bioeng Biotechnol. 2020;8:681.
14. González-Gallardo C, Martínez-Atienza J, Mataix B, Muñoz-Ávila JI, Daniel Martínez-Rodríguez J, Medialdea S, et al. Successful restoration of corneal surface integrity with a tissue-engineered allogeneic implant in severe keratitis patients. Biomed Pharmacother. 2023;162: 114612.
15. González-Andrades M, Garzón I, Gascón MI, Muñoz-Avila JI, Sánchez-Quevedo MC, Campos A, et al. Sequential development of intercellular junctions in bioengineered human corneas. J Tissue Eng Regen Med. 2009;3:442–9.
16. Garzón I, Martín-Piedra MA, Alfonso-Rodríguez C, González-Andrades M, Carriel V, Martínez-Gómez C, et al. Generation of a biomimetic human artificial cornea model using Wharton's jelly mesenchymal stem cells. Invest Ophthalmol Vis Sci. 2014;55:4073–83.
17. Blanco-Elices C, Morales-Álvarez C, Chato-Astrain J, González-Gallardo C, Ávila-Fernández P, Campos F, et al. Development of stromal differentiation patterns in heterotypical models of artificial corneas generated by tissue engineering. Front Bioeng Biotechnol. 2023;11:1124995.
18. Ionescu AM, Alaminos M, de la Cruz Cardona J, de Dios García-López Durán J, González-Andrades M, Ghinea R, et al. Investigating a novel nanostructured fibrin-agarose biomaterial for human cornea tissue engineering: rheological properties. J Mech Behav Biomed Mater. 2011;4:1963–73.
19. Ionescu AM, de la Cruz CJ, González-Andrades M, Alaminos M, Campos A, Hita E, et al. UV absorbance of a bioengineered corneal stroma substitute in the 240–400 nm range. Cornea. 2010;29:895–8.
20. Cardona J de la C, Ionescu A-M, Gómez-Sotomayor R, González-Andrades M, Campos A, Alaminos M, et al. Transparency in a fibrin and fibrin-agarose corneal stroma substitute generated by tissue engineering. Cornea. 2011;30:1428–35.
21. Vela-Romera A, Carriel V, Martín-Piedra MA, Aneiros-Fernández J, Campos F, Chato-Astrain J, et al. Characterization of the human ridged and non-ridged skin: a comprehensive histological, histochemical and immunohistochemical analysis. Histochem Cell Biol. 2019;151:57–73.
22. Martín-Cano F, Garzón I, Marañés C, Liceras E, Martín-Piedra MA, Ruiz-Montes AM, et al. Histological and immunohistochemical changes in the rat oral mucosa used as an autologous urethral graft. J Pediatr Surg. 2013;48:1557–64.
23. Bakopoulou A. Prospects of advanced therapy medicinal products-based therapies in regenerative dentistry: current status, comparison with global trends in medicine, and future perspectives. J Endod. 2020;46:S175–88.
24. Mathew JH, Bergmanson JPG, Doughty MJ. Fine structure of the interface between the anterior limiting lamina and the anterior stromal fibrils of the human cornea. Invest Ophthalmol Vis Sci. 2008;49:3914–8.
25. Meek KM, Knupp C, Lewis PN, Morgan SR, Hayes S. Structural control of corneal transparency, refractive power and dynamics. Eye (Lond). 2024. https://doi.org/10.1038/s41433-024-02969-7.
26. Yun SH, Chernyak D. Brillouin microscopy: assessing ocular tissue biomechanics. Curr Opin Ophthalmol. 2018;29:299–305.
27. Hanlon SD, Behzad AR, Sakai LY, Burns AR. Corneal stroma microfibrils. Exp Eye Res. 2015;132:198–207.
28. Werner S, Keller L, Pantel K. Epithelial keratins: biology and implications as diagnostic markers for liquid biopsies. Mol Aspects Med. 2020;72: 100817.
29. Fernanda de Mello Costa M, Weiner AI, Vaughan AE. Basal-like progenitor cells: a review of dysplastic alveolar regeneration and remodeling in lung repair. Stem Cell Reports. 2020;15:1015–25.
30. Jester JV. Corneal crystallins and the development of cellular transparency. Semin Cell Dev Biol. 2008;19:82–93.
31. Ramos T, Scott D, Ahmad S. An update on ocular surface epithelial stem cells: cornea and conjunctiva. Stem Cells Int. 2015;2015: 601731.
32. Yoshida S, Shimmura S, Kawakita T, Miyashita H, Den S, Shimazaki J, et al. Cytokeratin 15 can be used to identify the limbal phenotype in normal and diseased ocular surfaces. Invest Ophthalmol Vis Sci. 2006;47:4780–6.
33. Schlötzer-Schrehardt U, Kruse FE. Identification and characterization of limbal stem cells. Exp Eye Res. 2005;81:247–64.
34. Shaharuddin B, Harvey I, Ahmad S, Ali S, Meeson A. Characterisation of human limbal side population cells isolated using an optimised protocol from an immortalised epithelial cell line and primary limbal cultures. Stem Cell Rev Rep. 2014;10:240–50.
35. Gouveia RM, Vajda F, Wibowo JA, Figueiredo F, Connon CJ. YAP, ΔNp63, and β-catenin signaling pathways are involved in the modulation of corneal epithelial stem cell phenotype induced by substrate stiffness. Cells. 2019;8:347.
36. Hopkinson A, Notara M, Cursiefen C, Sidney LE. Increased anti-inflammatory therapeutic potential and progenitor marker expression of corneal mesenchymal stem cells cultured in an optimized propagation medium. Cell Transplant. 2024;33:9636897241241992.
37. Na KS, Mok JW, Joo C-K. Ex vivo human corneal epithelial cell expansion from a xeno-feeder-free system. Ophthalmic Res. 2015;53:217–24.
38. Seo BR, Chen X, Ling L, Song YH, Shimpi AA, Choi S, et al. Collagen microarchitecture mechanically controls myofibroblast differentiation. Proc Natl Acad Sci U S A. 2020;117:11387–98.
39. Pellegrini G, Ardigò D, Milazzo G, Iotti G, Guatelli P, Pelosi D, et al. Navigating market authorization: the path Holoclar took to become the first stem cell product approved in the European Union. Stem Cells Transl Med. 2018;7:146–54.
40. Nureen L, Di Girolamo N. Limbal epithelial stem cells in the diabetic cornea. Cells. 2023;12:2458.
41. Alaminos M. Quantitative results of the analysis of human native and bioengineered tissues corresponding to the work "Histological, histochemical and immunohistochemical characterization of NANOULCOR nanostructured fibrin-agarose human cornea substitutes generated by tissue engineering." 2024. Zenodo. https://doi.org/10.5281/zenodo.10845879.

Publisher's Note